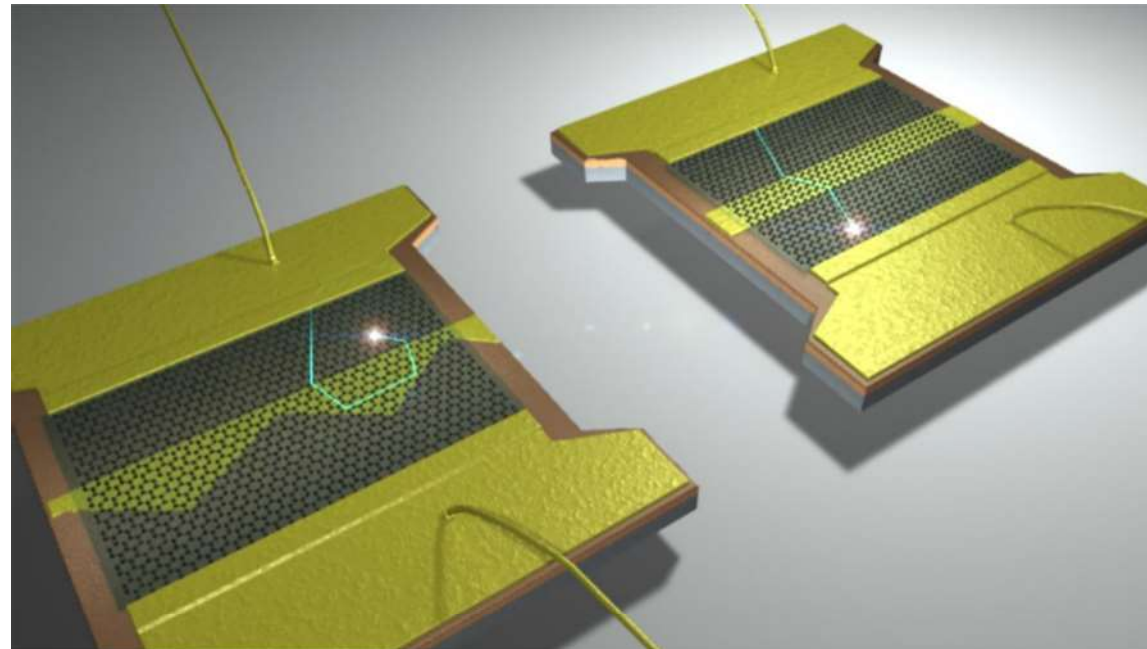


Probing electron optics in a Dirac fermion reflector

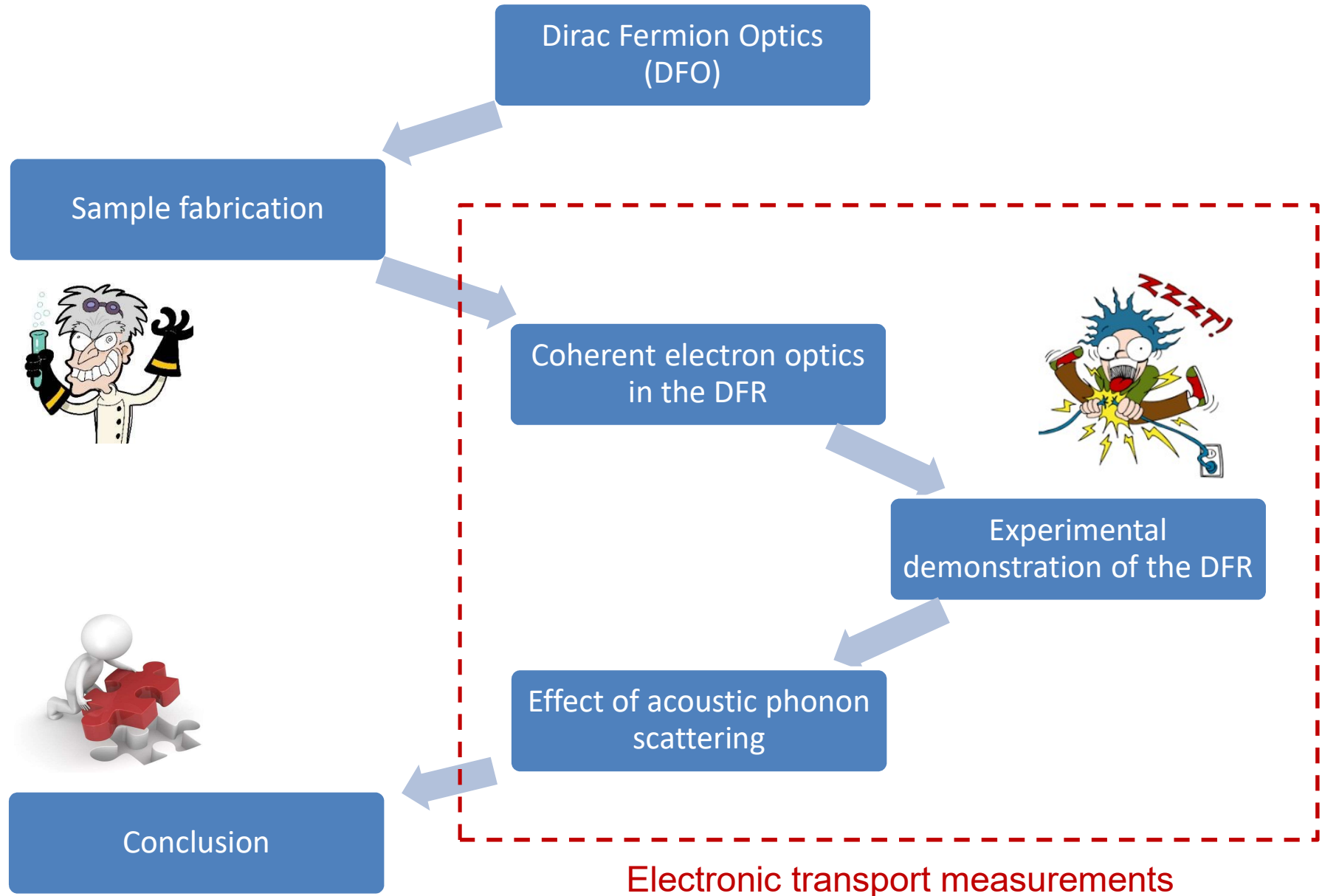


H. Graef^{1,2}, M. Rosticher¹, D. Mele¹, Q. Wilmart¹, L. Banszerus³, C. Stampfer³, T. Taniguchi⁴, K. Watanabe⁴, E. Bocquillon¹, G. Fève¹, J.M. Berroir¹, E.H.T. Teo² and B. Plaçais¹

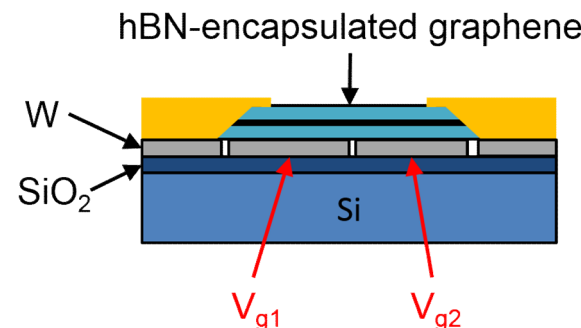
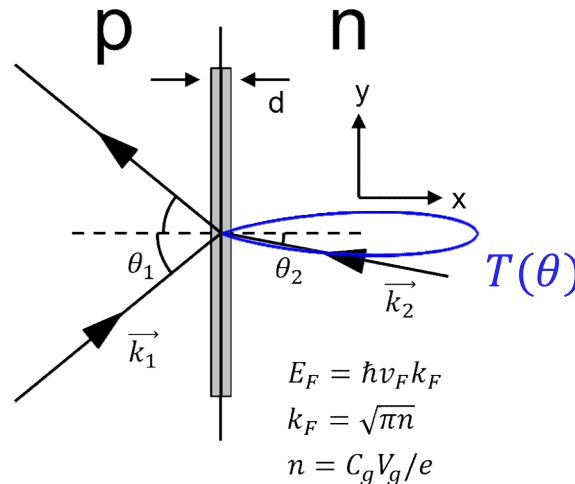
¹Laboratoire Pierre Aigrain – ENS, Paris, France; ²CINTRA – Nanyang Technological University, Singapore; ³2nd Institute of Physics A – RWTH Aachen, Germany;

⁴National Institute for Materials Science, Tsukuba, Japan

Outline

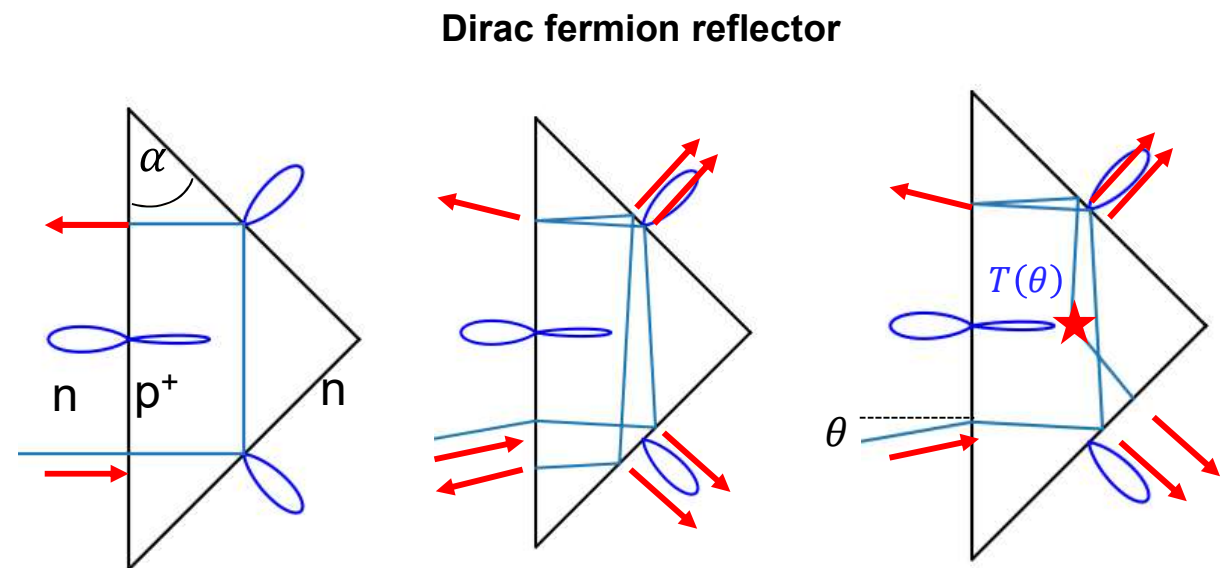
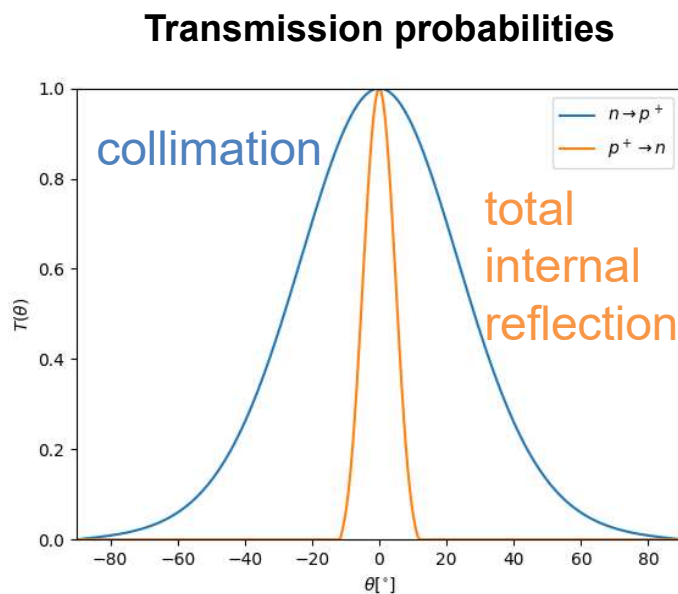


Dirac Fermion Optics (DFO)



	Photon optics (3D)	Dirac fermion optics (2D)
Medium	transparent	ballistic
Phase velocity	$3 \cdot 10^8 \text{ ms}^{-1}$	10^6 ms^{-1}
Snell-Descartes	$n_1 \sin \theta_1 = n_2 \sin \theta_2$	$E_{F1} \sin \theta_1 = E_{F2} \sin \theta_2$
Critical angle	$\theta_c = \arcsin \left(\frac{n_2}{n_1} \right)$	$\theta_c = \arcsin \left(\frac{E_{F2}}{E_{F1}} \right)$
Fresnel relation	$R_s = \left \frac{n_1 \cos \theta_i - n_2 \cos \theta_t}{n_1 \cos \theta_i + n_2 \cos \theta_t} \right ^2$	$T(\theta) = e^{-\pi \frac{2d}{ k_1 - k_2 } k_2^2 \sin^2 \theta}$

Dirac Fermion Reflector (DFR)

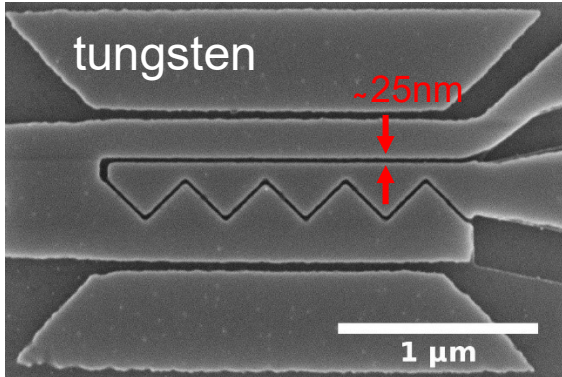


Q. Wilmart et al., 2D Mat. **1** (2014) 11006





Sample fabrication

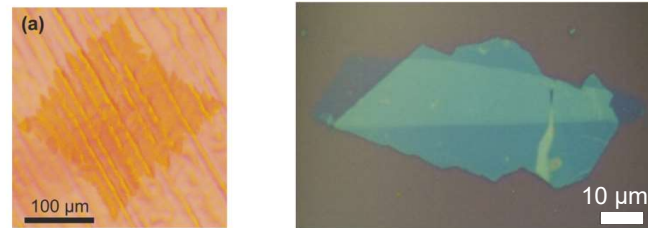


nano-patterned bottom gates

- gold or tungsten
- made using EBL+RIE
- independent control
- of E_{F1} and E_{F2}
- sharp junction $k_F d \lesssim 1$
- small device $L < l_{mfp}$

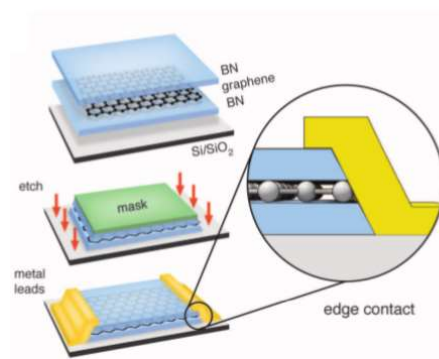
Morikawa et al., Semicond. Sci. Technol. **32** (2017) 045010
20° opening angle, top-bottom gate approach:

monocrystalline CVD graphene encapsulated in exfoliated hBN



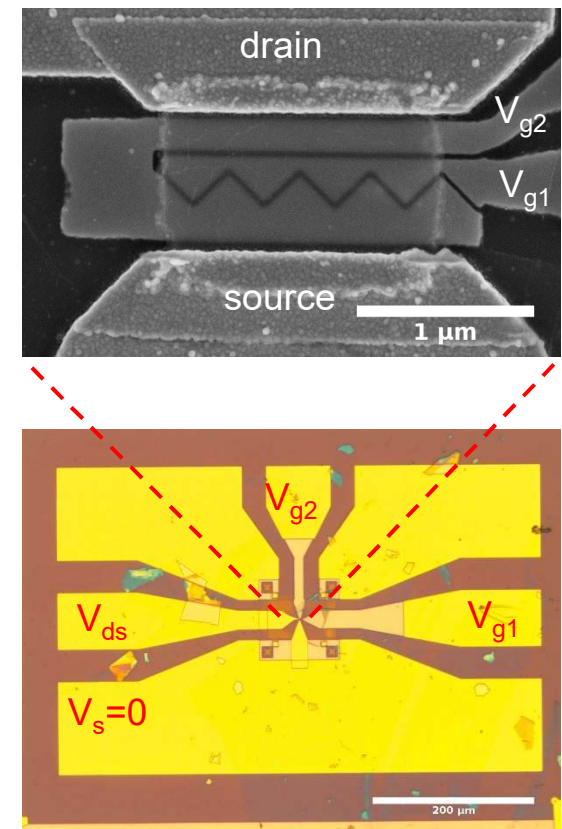
L. Banszerus et al.,
Nano Lett. **16** (2016) 1387

etching + 1D edge contact

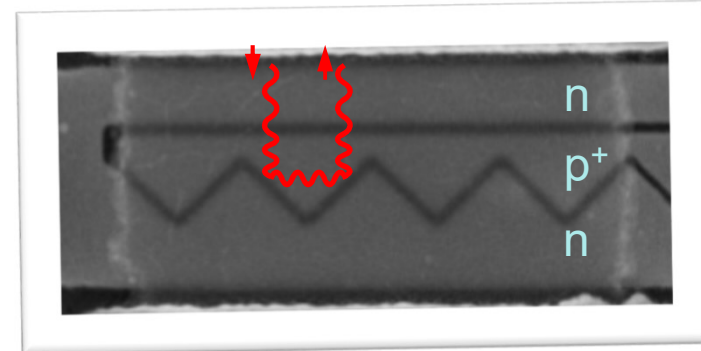
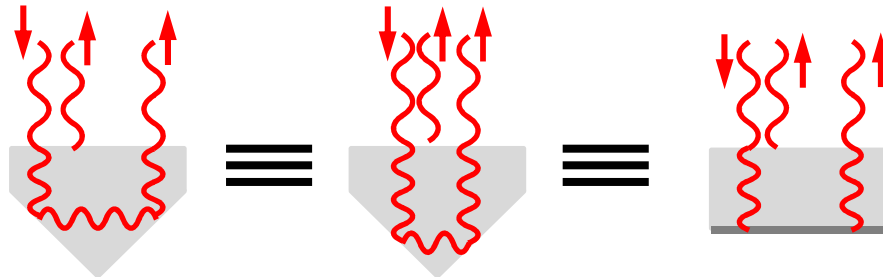


Wang et al., Science **342** (2013) 614

final sample



- nano-patterned bottom gates ensure precise control of the refractive index
- high-quality encapsulated graphene ensures long mean free path

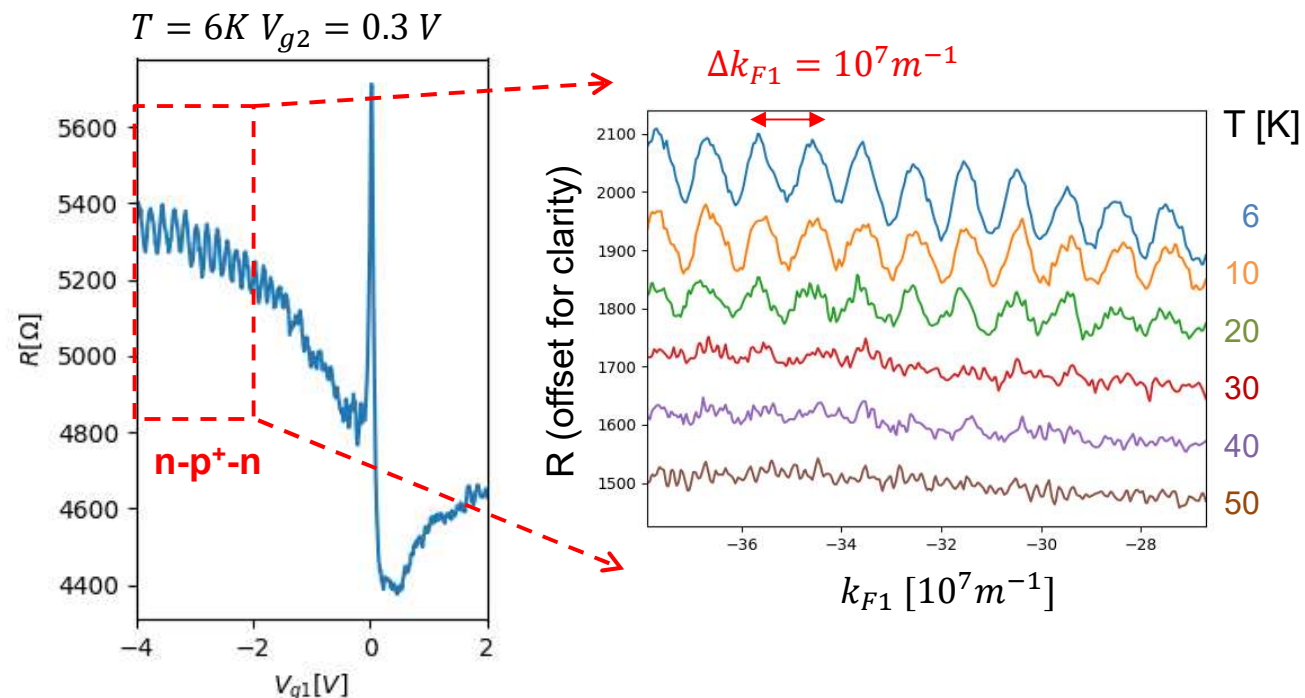


Calibrate gate coupling, so that:

$$L = \frac{2\pi}{\Delta k_{F1}} = 600 \text{ nm}$$

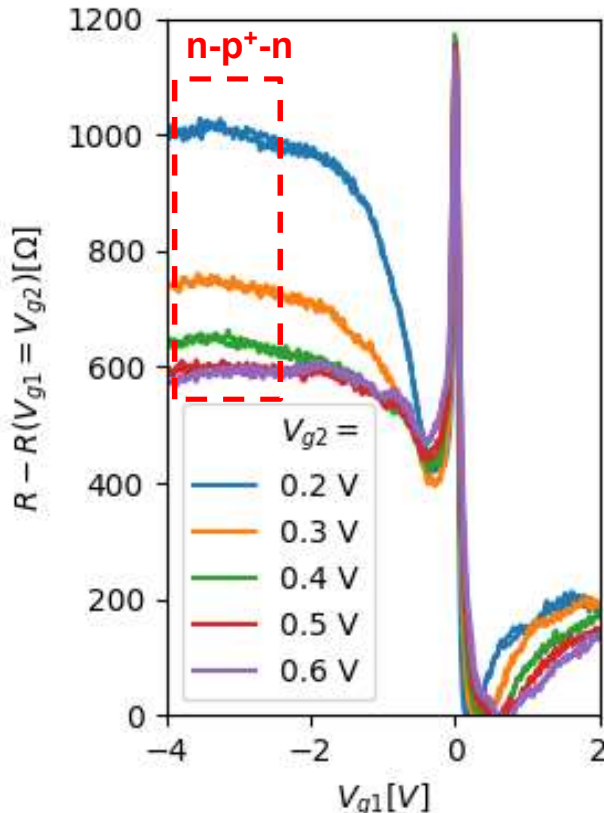
Oscillations disappear around:

$$T_{smear} = \frac{\hbar v_F}{2k_B \cdot 600 \text{ nm}} = 40 \text{ K}$$

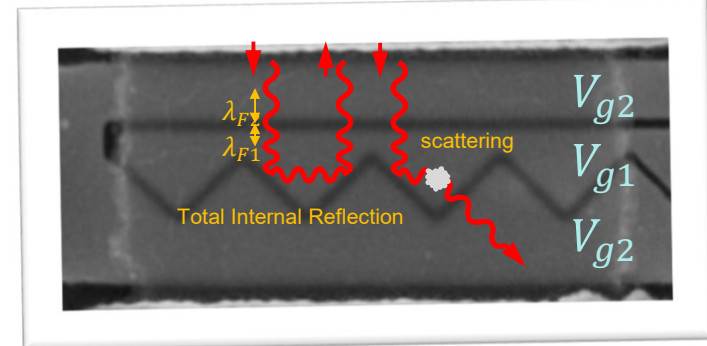
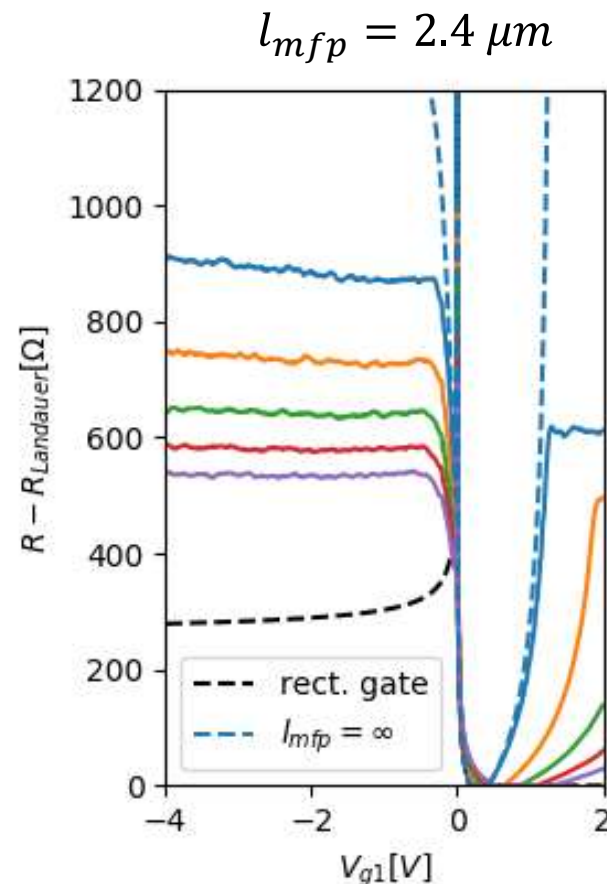


➤ Calibration of the DFR dwell length at 600 nm

DC experiment at 60K



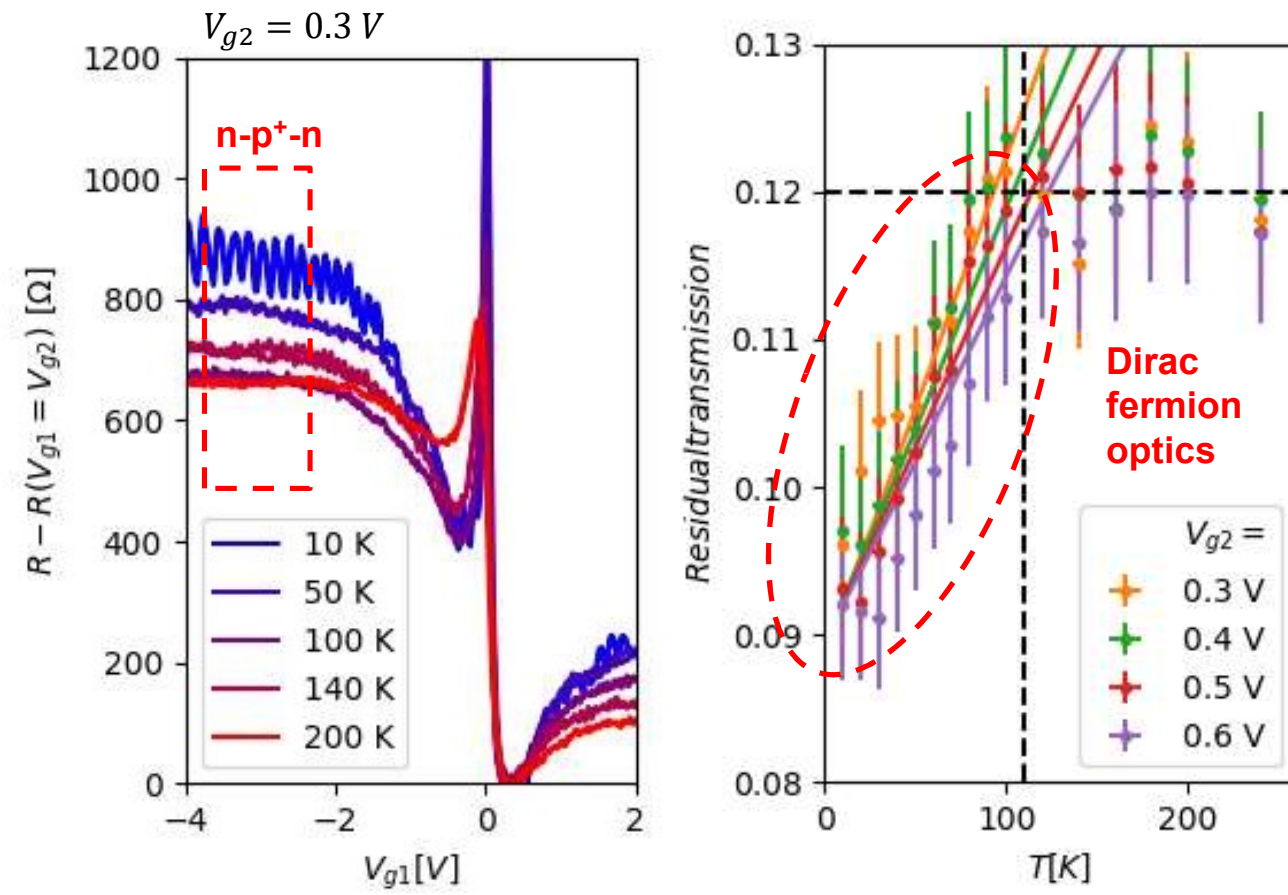
Scattering simulation



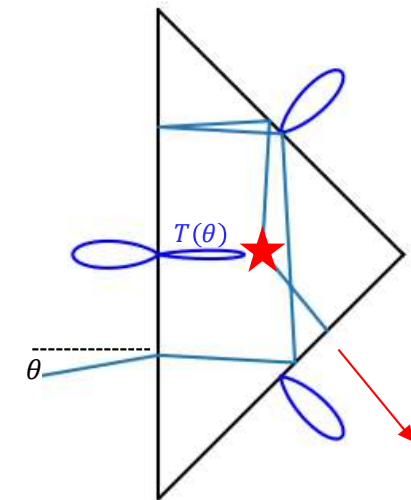
- in situ tuning of the DFO refractive index
- up to $E_{F1}/E_{F2} = -4.8$ ($\theta_c = 12^\circ$)
- c.f. diamond/air: 2.4

- DFR = resistance plateau in the n-p+ regime
- also works at 10 GHz

Effect of acoustic phonon scattering



$$\frac{1}{R} = \frac{4e^2}{h} \frac{k_{F2}W}{\pi} \langle T(\theta) \rangle_\theta$$



$$l_{phonon} = \frac{300 \text{ K}}{T} \cdot 800 \text{ nm}$$

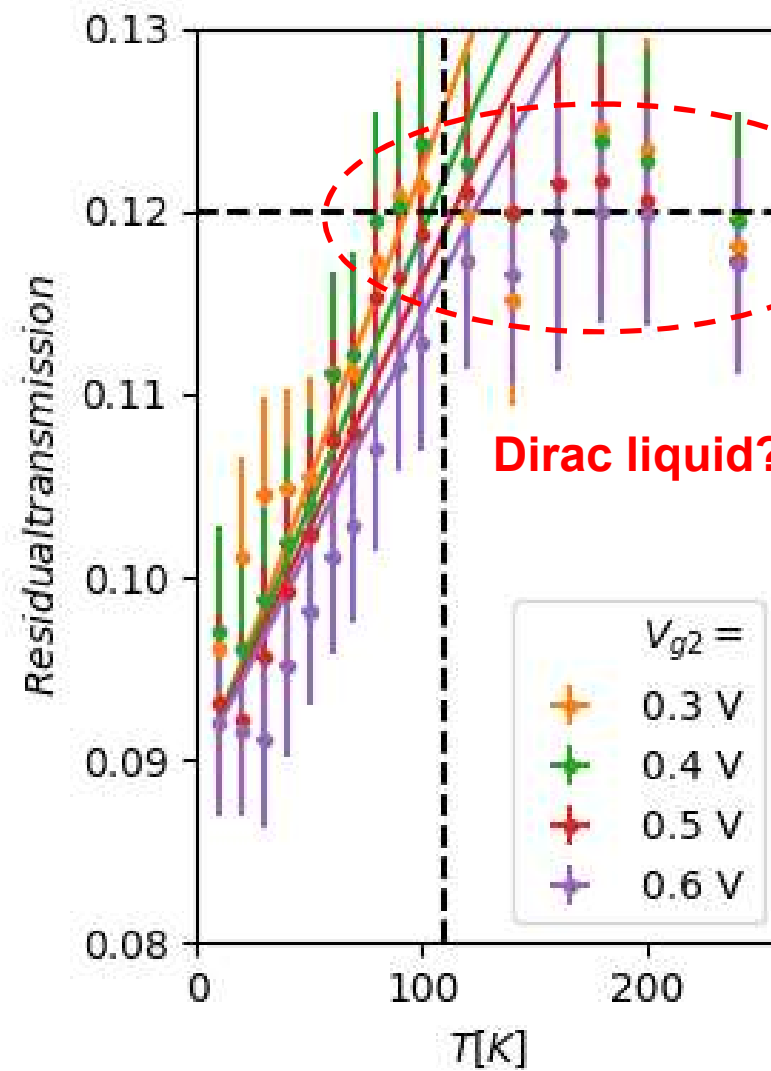
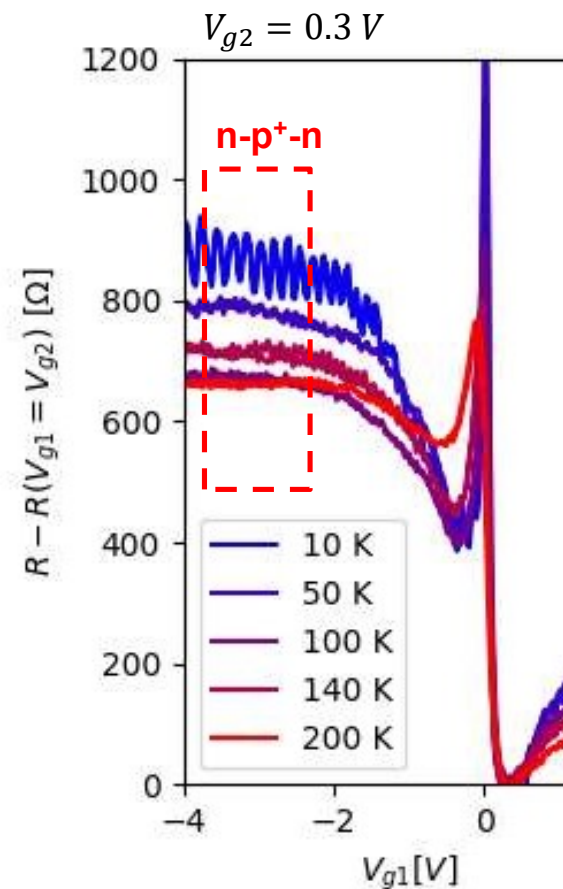
Hwang & Das Sarma, PRB 77 (2008) 115449

$$T(\theta) = e^{-\pi \frac{2d}{|k_1 - k_2|} k_2^2 \sin^2 \theta}$$

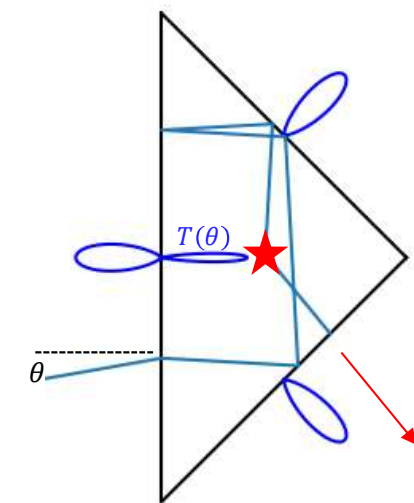
$$T_{DFR} = \int_{-\pi/2}^{+\pi/2} T(\theta) (1 - T(\theta))^{l_{phonon}/L} \cos(\theta) d\theta$$

- Acoustic phonon model explains T-dependence quantitatively

Effect of acoustic phonon scattering



$$\frac{1}{R} = \frac{4e^2}{h} \frac{k_{F2}W}{\pi} \langle T(\theta) \rangle_\theta$$



$$phonon = \frac{300 \text{ K}}{T} \cdot 800 \text{ nm}$$

wang & Das Sarma, PRB 77 (2008) 115449

$$T(\theta) = e^{-\pi \frac{2d}{|k_1 - k_2|} k_2^2 \sin^2 \theta}$$

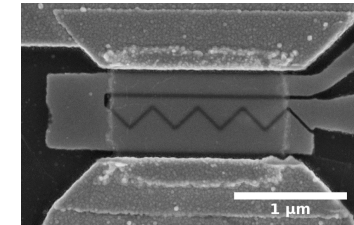
$$T_{DFR} = \int_{-\pi/2}^{+\pi/2} T(\theta) (1$$

- Acoustic phonon model explains T-dependence quantitatively

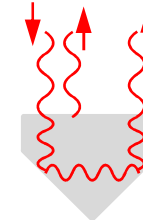
Conclusions



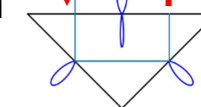
- ✓ nano-patterned gates enable local **control of DFO refractive index**



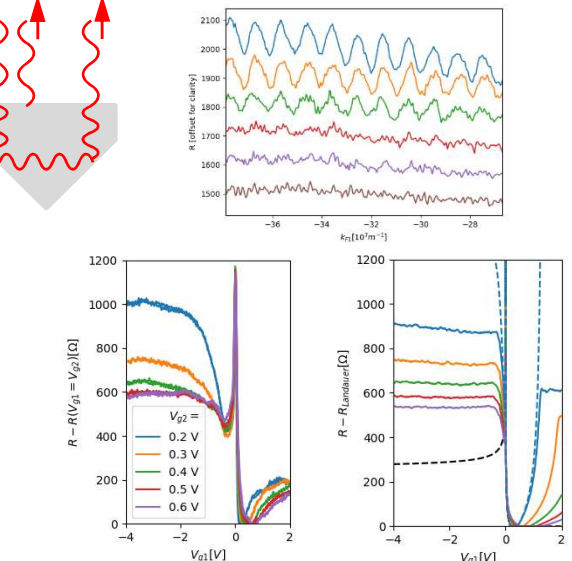
- ✓ **coherent DFO** calibrates length of the reflector



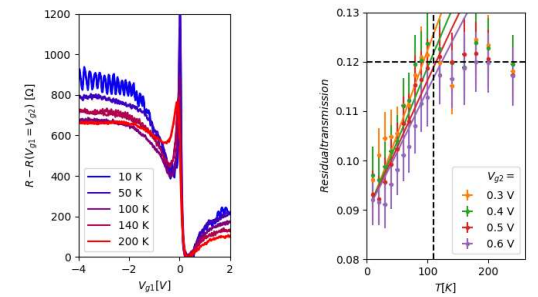
- ✓ **geometric DFO effect confirmed** (DC and 10 GHz) and in quantitative agreement with scattering simulation



- ✓ temperature dependence in quantitative agreement with **acoustic phonon scattering model**



- ✓ **viscous Dirac liquid above 100 K ?**



➤ Thank you for your attention!